

# Atmospheric Chemistry and Physics

Supporting Information

**Identification and characterization of aging products in the glyoxal/ammonium sulfate system - Implications for light-absorbing material in atmospheric aerosols**

Christopher J. Kampf<sup>1</sup>, Ronit Jakob<sup>1</sup>, and Thorsten Hoffmann<sup>1</sup>

<sup>1</sup> Institute for Inorganic and Analytical Chemistry, Johannes Gutenberg-University, Mainz, Germany

Correspondance to: Thorsten Hoffmann ([hoffmant@uni-mainz.de](mailto:hoffmant@uni-mainz.de))

## List of experiments

A selected list of experiments conducted for this work can be found in Table S1.

Table S1: Selected list of experiments

Experiments of glyoxal/AS reaction products and kinetics				
Measurement	[Gly] /mol L <sup>-1</sup>	[Salt] /mol L <sup>-1</sup>	Comment	
1	HPLC-DAD-ESI-MS/MS	0.01	3 (AS)	Initial kinetics and products
2	HPLC-DAD-ESI-MS/MS	0.3	3 (AS)	Kinetics and products
3	HPLC-DAD-ESI-MS/MS	0.9	3 (AS)	Kinetics and products
4	HPLC-DAD-ESI-MS/MS	1.5	3 (AS)	Kinetics and products
5	HPLC-DAD-ESI-MS/MS	1.5	3 (AN)	Kinetics and products
6	HPLC-DAD-ESI-MS/MS	1.5	3 (AS)	Products MS/MS
7	HPLC-DAD-ESI-MS/MS	1.5	3 (AN)	Products MS/MS
Supplementary tests to support Figure 1 in the main text and product identification				
Measurement	Species and concentration		Comment	
8	HPLC-DAD-ESI-MS	10 $\mu$ M – 1mM BI	Calibration curve	
9	HPLC-DAD-ESI-MS/MS	3 M AS	Background	
10	HPLC-DAD-ESI-MS/MS	H <sub>2</sub> O	Background	
11	HPLC-DAD-ESI-MS/MS	0.02 M Gly	UV and MS characterization	
12	HPLC-DAD-ESI-MS/MS	0.02 M IM	UV and MS characterization	
13	HPLC-DAD-ESI-MS/MS	0.02 M IC	UV and MS characterization	
14	HPLC-DAD-ESI-MS/MS	0.02 M IM + 0.02 M Gly	UV and MS characterization	
15	HPLC-DAD-ESI-MS/MS	0.02 M IC + 0.02 M Gly	UV and MS characterization	
16	HPLC-DAD-ESI-MS/MS	0.02 M BI + 0.02 M Gly	UV and MS characterization	
17	HPLC-DAD-ESI-MS/MS	0.2 mM IC, 3 M AS	Ionization efficiency test	
18	HPLC-DAD-ESI-MS/MS	0.02 M IC, 3 M AS	Products	

AS = ammonium sulfate, AN = ammonium nitrate, Gly = glyoxal, BI = 2,2'-biimidazole, IM = 1H-imidazole, IC = 1H-imidazole-2-carboxaldehyde

## Characterization of prominent reaction products in the glyoxal/ammonium sulfate system using HPLC-ESI-MS/MS

Figures S1 to S9 show HPLC-ESI-MS/MS data for the characterization of monocyclic and bicyclic imidazoles from standard solutions. In each figure the upper part represents the extracted ion chromatogram (EIC), the MS spectrum is shown in the middle, and the lower part depicts the MS/MS spectrum of the respective compound.

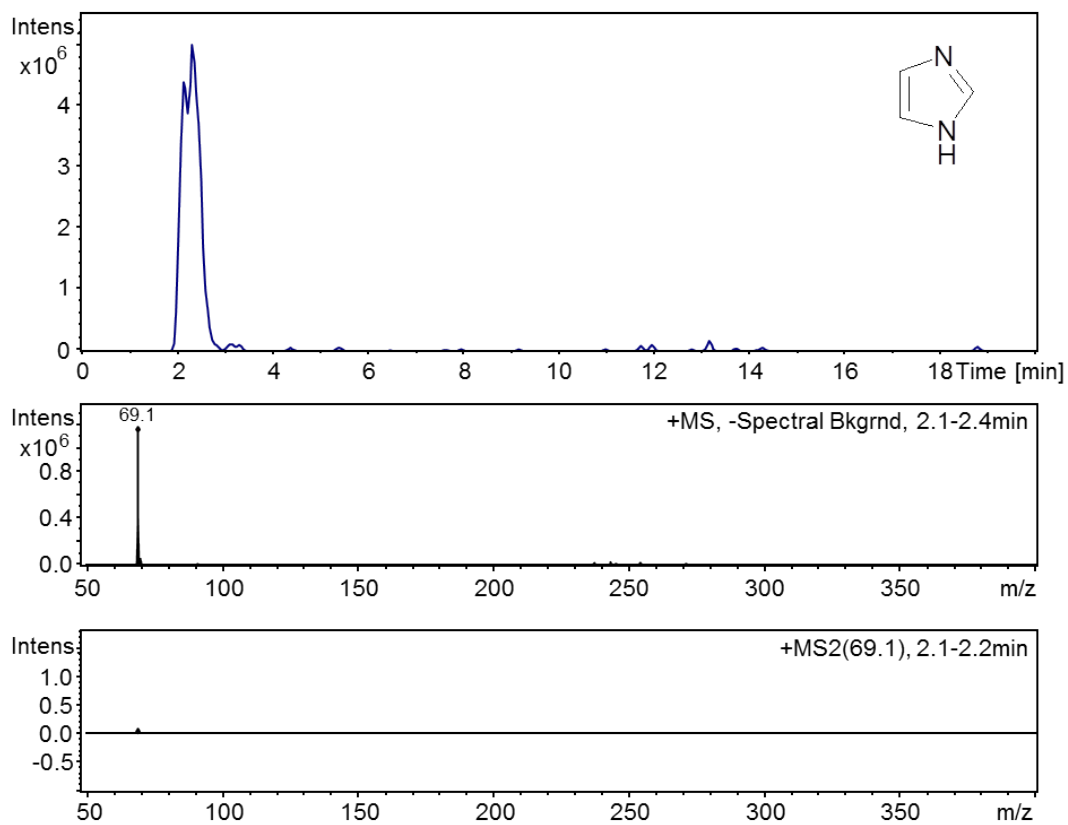


Figure S1: Chromatographic and mass spectrometric characterization of 1H-imidazole (IM).

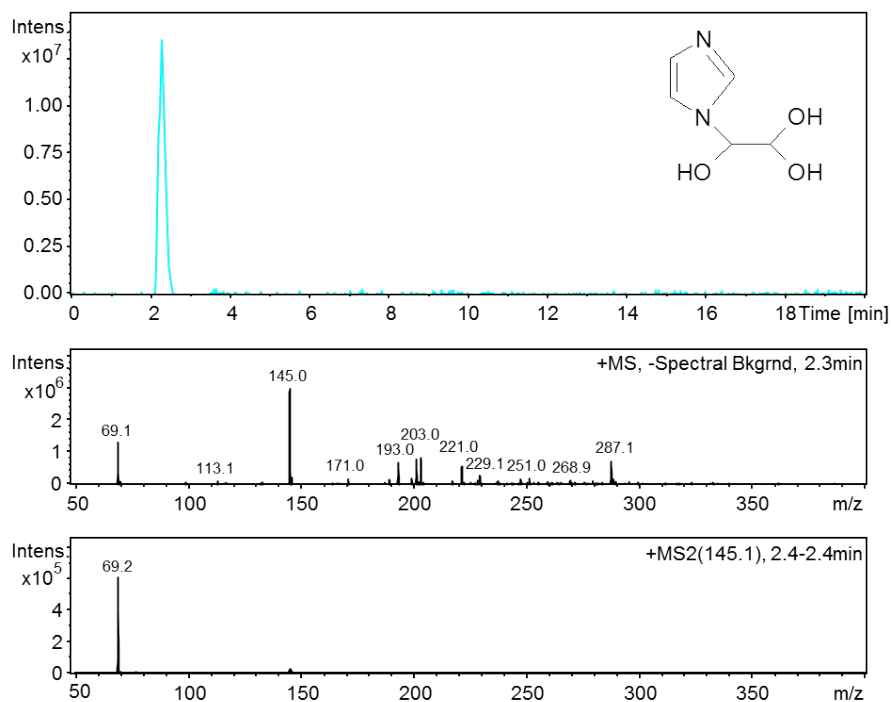


Figure S2: Chromatographic and mass spectrometric characterization of hydrated mono glyoxal substituted 1H-imidazole (HGI).

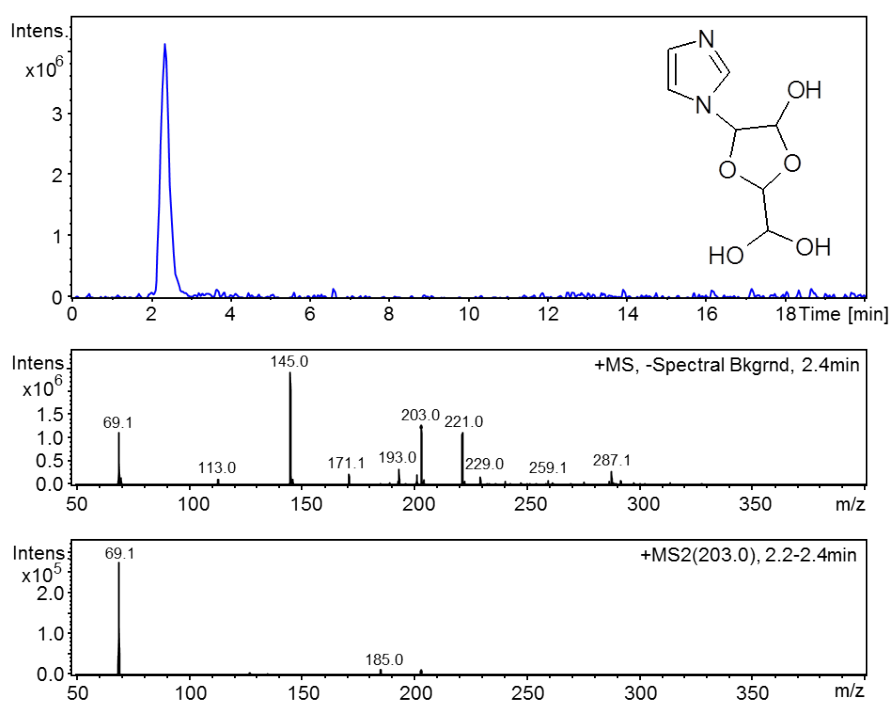


Figure S3: Chromatographic and mass spectrometric characterization of hydrated glyoxal dimer substituted 1H-imidazole (HGDI).

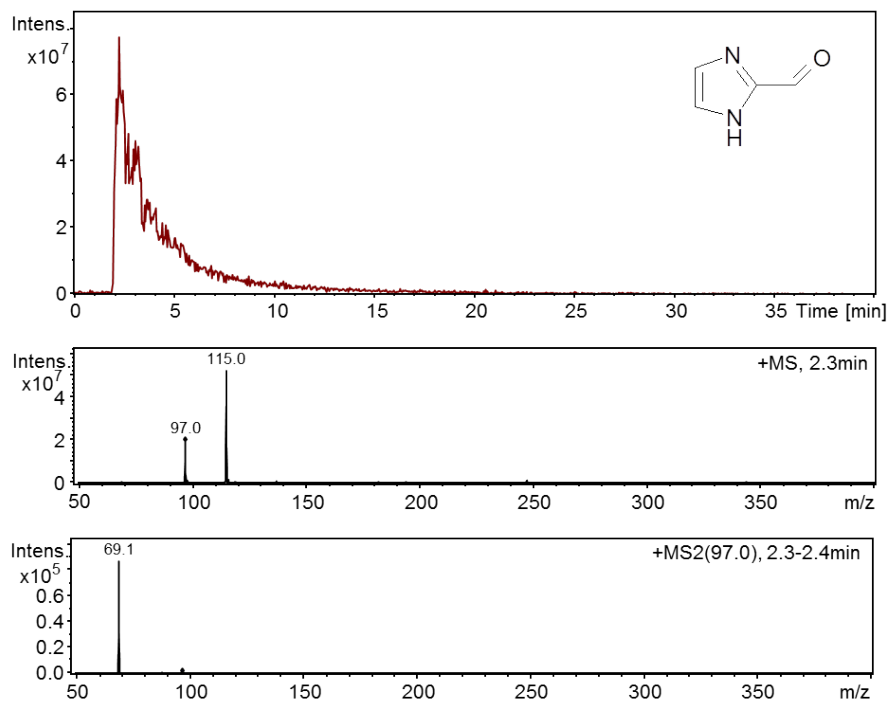


Figure S4: Chromatographic and mass spectrometric characterization of 1H-imidazole-2-carboxaldehyde (IC).

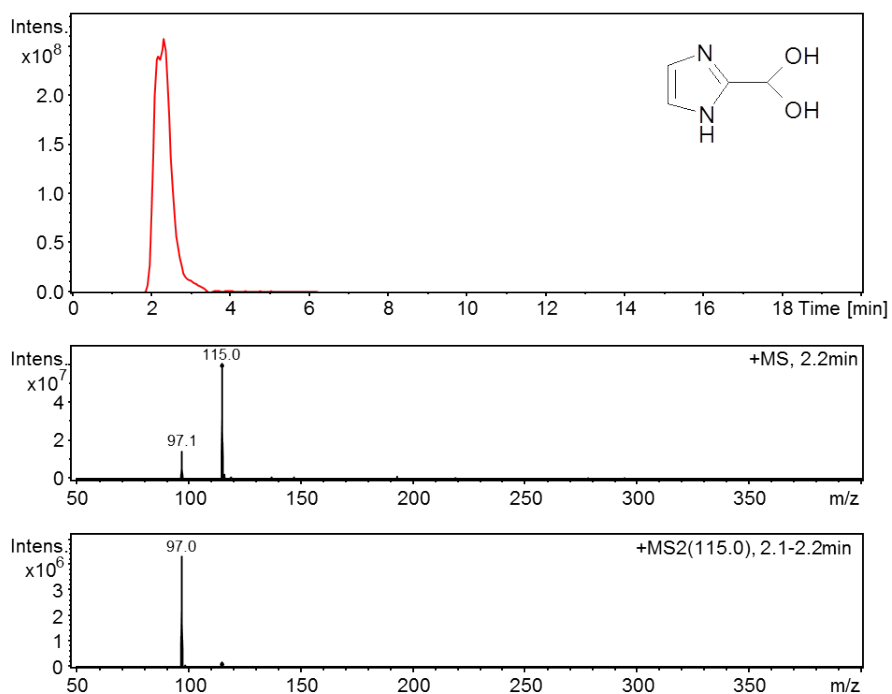


Figure S5: Chromatographic and mass spectrometric characterization of hydrated 1H-imidazole-2-carboxaldehyde (HIC).

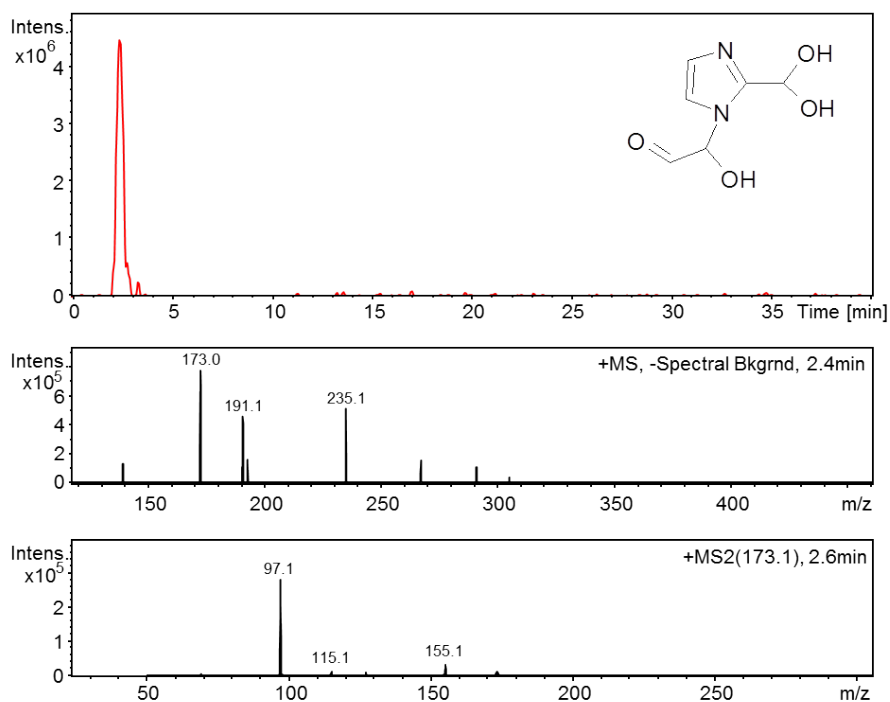


Figure S6: Chromatographic and mass spectrometric characterization of mono glyoxal substituted hydrated 1H-imidazole-2-carboxaldehyde (GHIC).

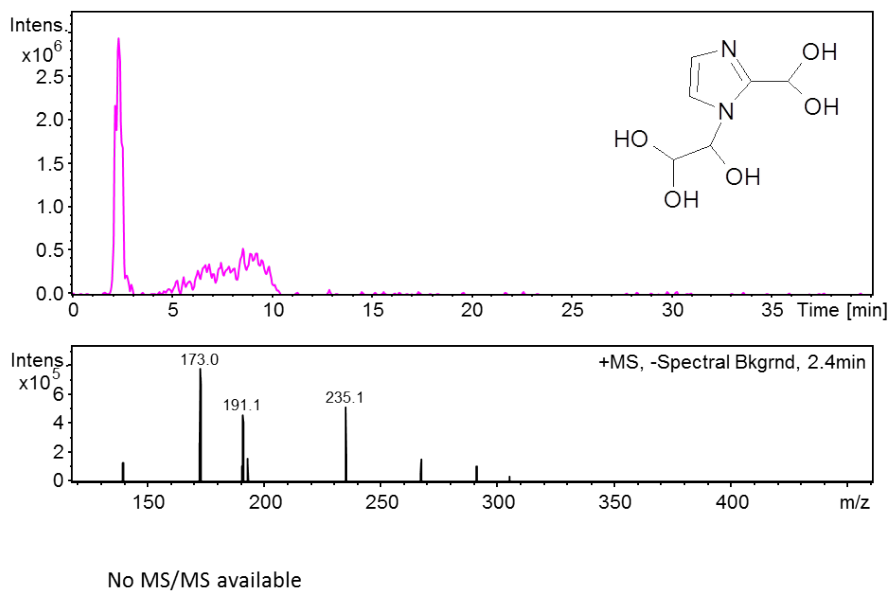


Figure S7: Chromatographic and mass spectrometric characterization of hydrated mono glyoxal substituted hydrated 1H-imidazole-2-carboxaldehyde (HGHIC).

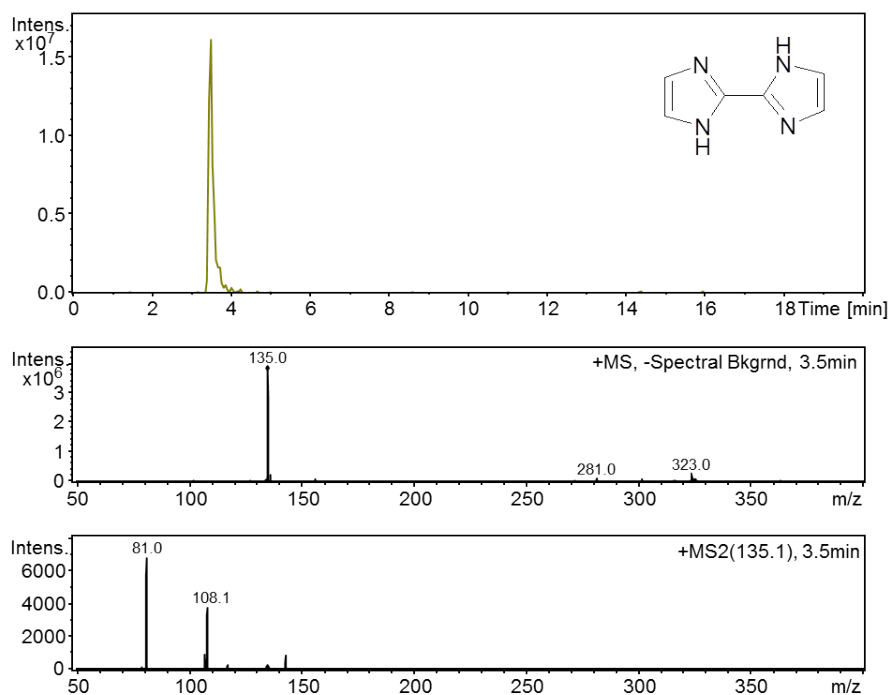


Figure S8: Chromatographic and mass spectrometric characterization of 2,2'-biimidazole (BI).

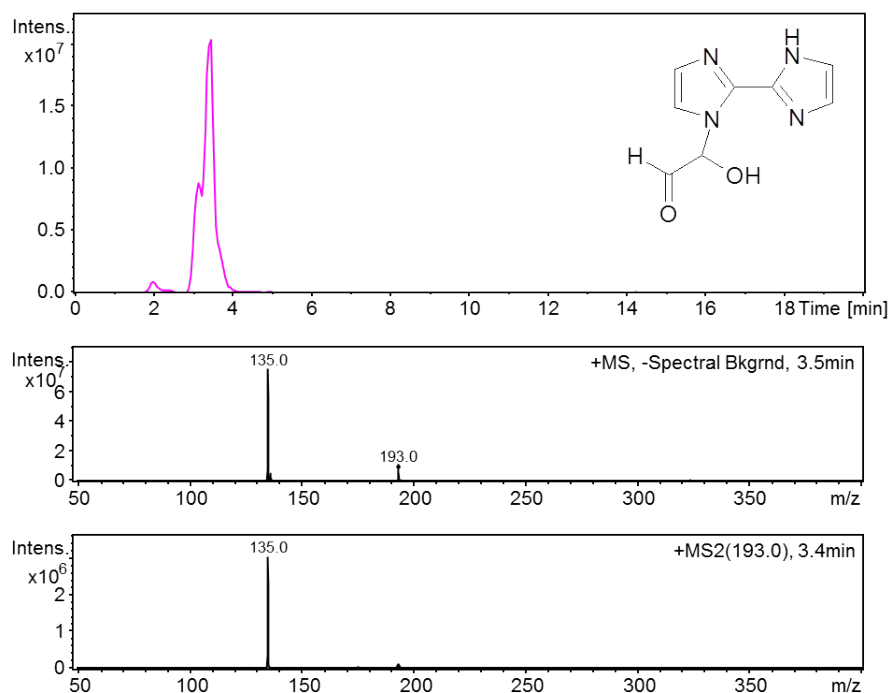


Figure S9: Chromatographic and mass spectrometric characterization of mono glyoxal substituted 2,2'-biimidazole (GBI).

## Determination of the molar extinction coefficient of BI

Figure S10 shows a linear fit of the concentration dependent absorbance of BI at 280 nm. The calibration curve was constructed using concentrations ranging from  $10\mu\text{M}$  –  $1\text{mM}$ . The linear fit parameters are listed in Table S2. Table S3 shows the calculations for the determination of the molar extinction coefficient of BI.

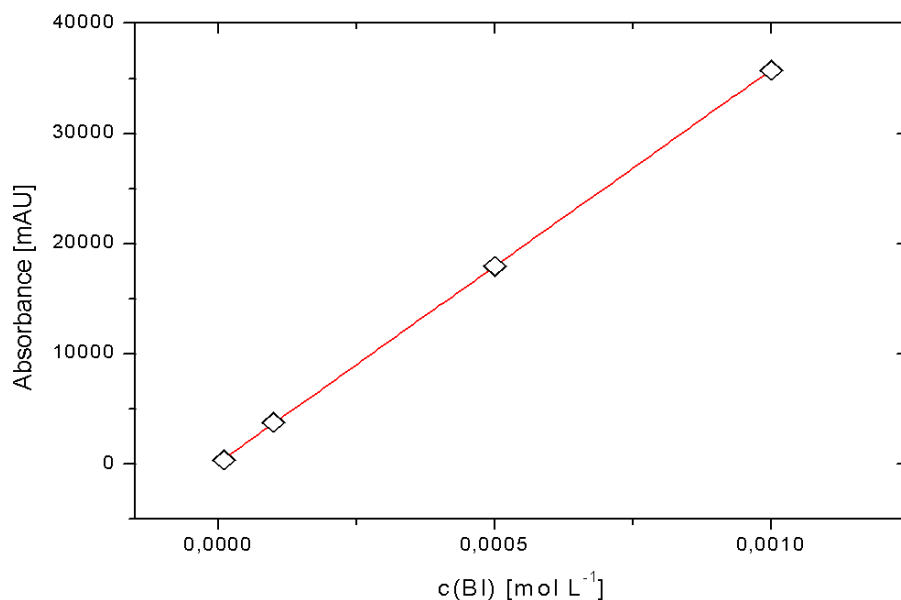


Figure S10: Linear fit of BI concentration dependent absorbance at 280 nm.

Table S2: Linear fit parameters of concentration dependent absorbance of BI in water at 280 nm.

		value	error
slope	$\times 10^7$	3.56	0.01
intercept	$\times 10^2$	1.18	0.73
Pearson R		0.99999	
adjusted R <sup>2</sup>		0.99996	
SSE*		2.08E4	

\* SSE = sum of squared residuals



Table S3: Determination of the molar extinction coefficient of BI.

pathlength /cm	[BI] /M	A /A.U.	$\epsilon$ /M <sup>-1</sup> cm <sup>-1</sup>
1	0.00001	0.373	37300
1	0.0001	3.777	37770
1	0.0005	17.974	35948
1	0.001	35.741	35741
mean value			36690
std. dev.			998

A = Absorbance,  $\epsilon$  = molar extinction coefficient

## Determination of the production rate of BI in 3M AS solutions for different initial Gly concentrations

Figure S11 shows linear fits to obtain initial production rates of BI in 3 M AS dependent on initial Gly concentration. Linear fit parameters are listed in Table S4. Figure S12 shows a zoom-in of BI production for 0.01 M initial glyoxal concentration.

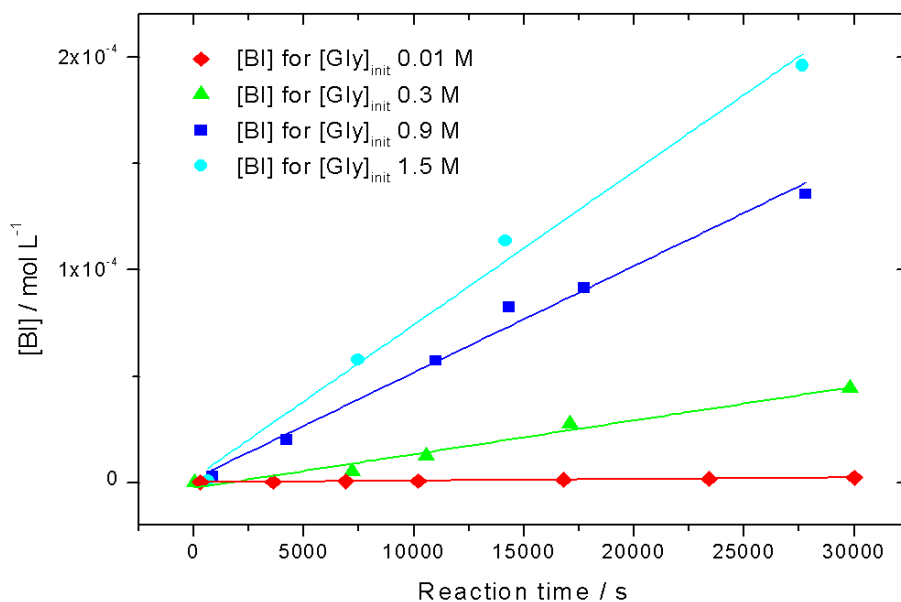


Figure S11: Linear fits of [BI] dependent on initial [Gly] to obtain initial production rates of BI in 3 M AS dependent on initial Gly concentration

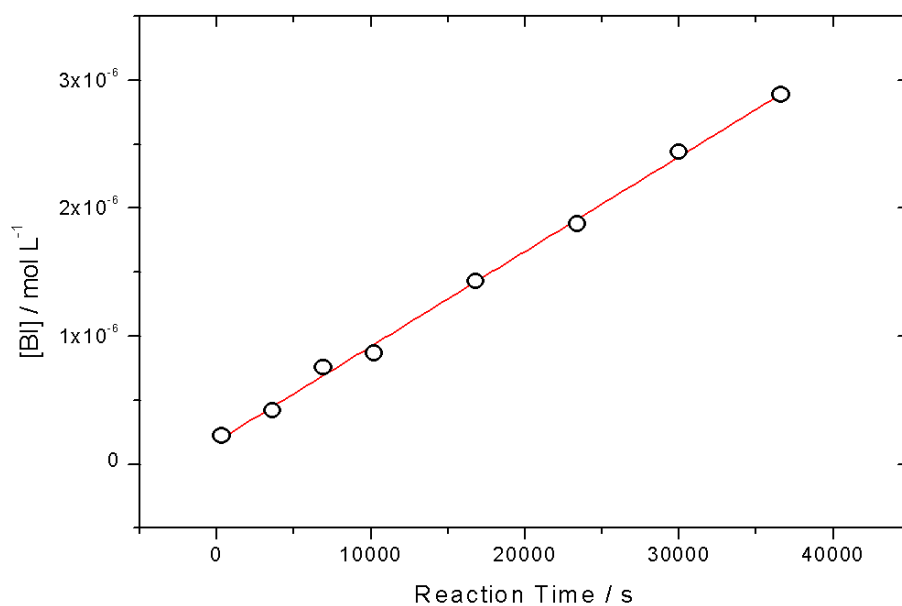


Figure S12: Linear fit of [BI] to obtain initial production rate of BI in 0.01 M glyoxal and 3 M AS.

Table S4: Linear fit parameters to obtain initial production rate of BI.

[Gly] <sub>init</sub> /M		0.01		0.3		0.9		1.5	
		value	error	value	error	value	error	value	error
slope	×10 <sup>-9</sup>	0.074	0.002	1.58	0.14	5.00	0.26	7.19	0.44
intercept	×10 <sup>-6</sup>	0.18	0.03	-2.40	2.40	1.82	4.01	2.34	7.11
Pearson R		0.99839		0.98773		0.99464		0.9962	
adjusted R <sup>2</sup>		0.99614		0.96747		0.98662		0.98862	
SSE*	×10 <sup>-10</sup>	0.0001		0.32		1.27		1.58	

\* SSE = sum of squared residuals

## Fast equilibrium between GBI and BI

The linear dependency between the concentrations of GBI and BI depending on the initial glyoxal concentration in the Gly/AS mixtures is illustrated in Figure S13.

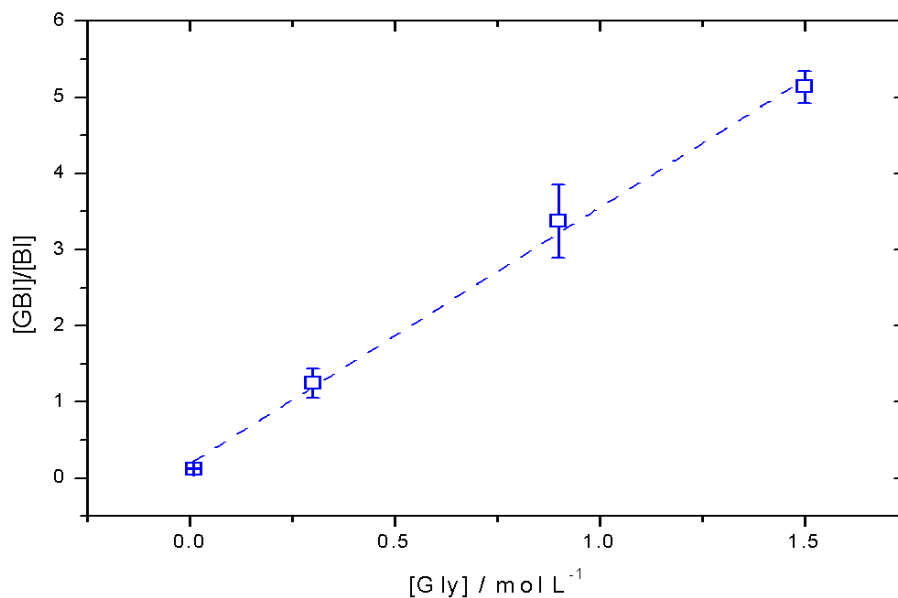


Figure S13: Dependence of  $[GBI]/[BI]$  observed during the first 10 h of reaction time from initial  $[Gly]$ .

## Selected 3D-UV chromatograms

The following figures S14 and S15 show selected measurements as 3D UV chromatograms. Retention times are on the x-axis, absorbing wavelengths are on the y-axis and absorption intensities are on the z-axis.

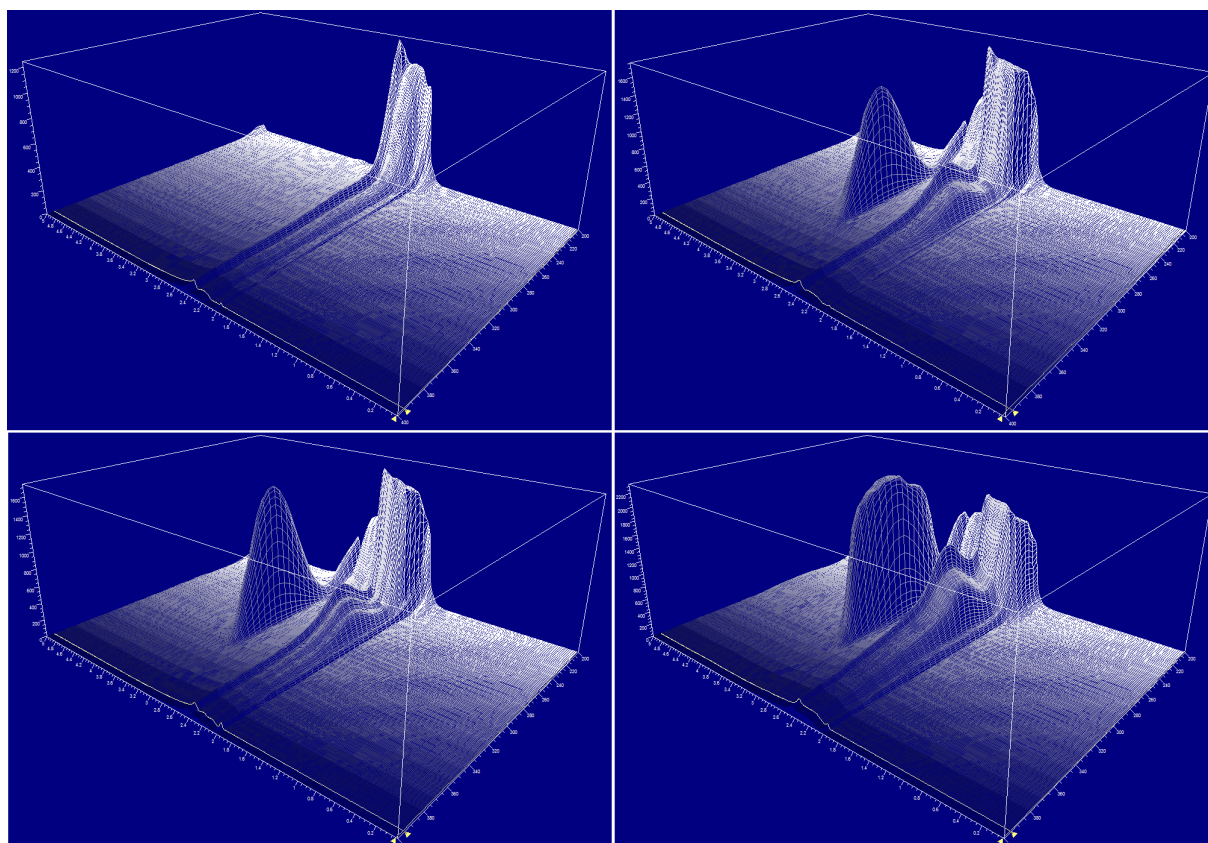


Figure S14: Temporal evolution of 3D UV chromatograms of 1.5 M Gly in 3 M AS. Upper left hand corner 0.15 h after preparation, upper right hand corner 15.0 h after preparation, lower left hand corner 16.1 h after preparation, lower right hand corner 147.5 h after preparation

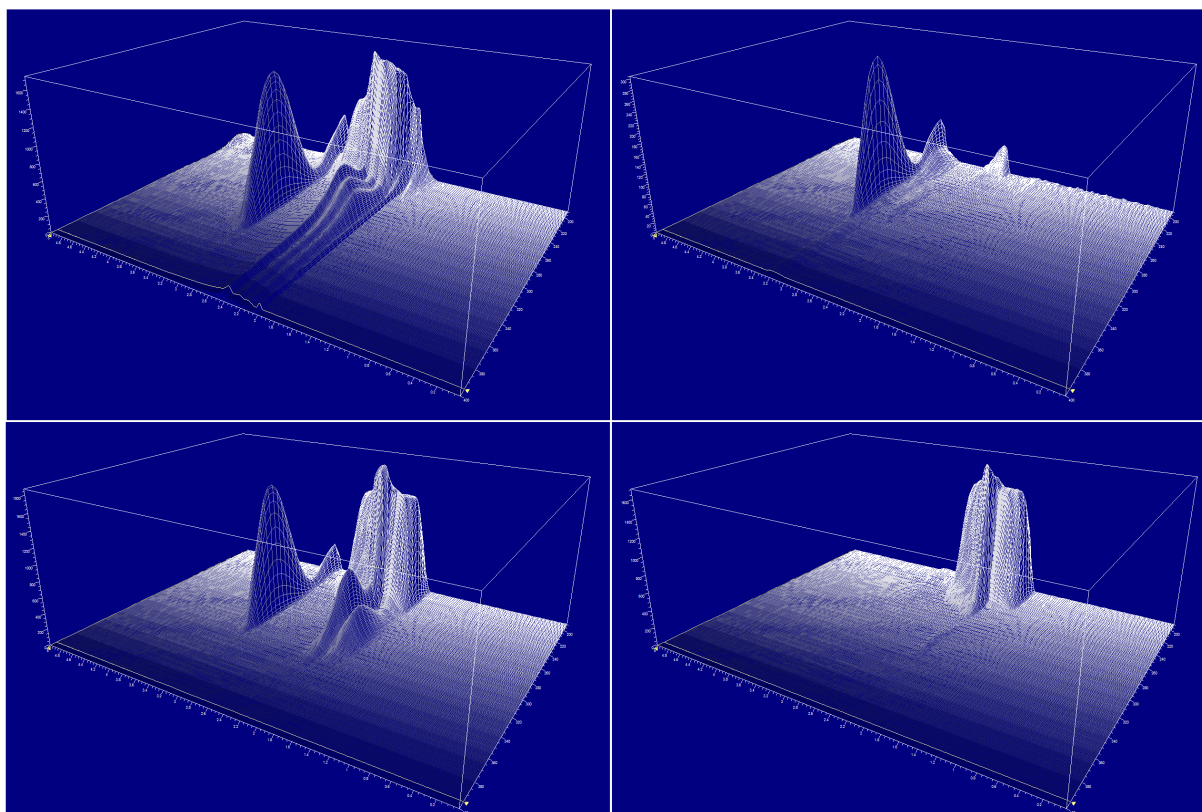


Figure S15: 3D UV chromatograms of 1.5 M Gly in 3 M AS (15 h after preparation, upper left hand corner) and standards: 0.04 mM BI standard (upper right hand corner), 0.02 M IC standard (lower left hand corner) and 0.02 M IM standard (lower right hand corner)

## UV-Vis spectra

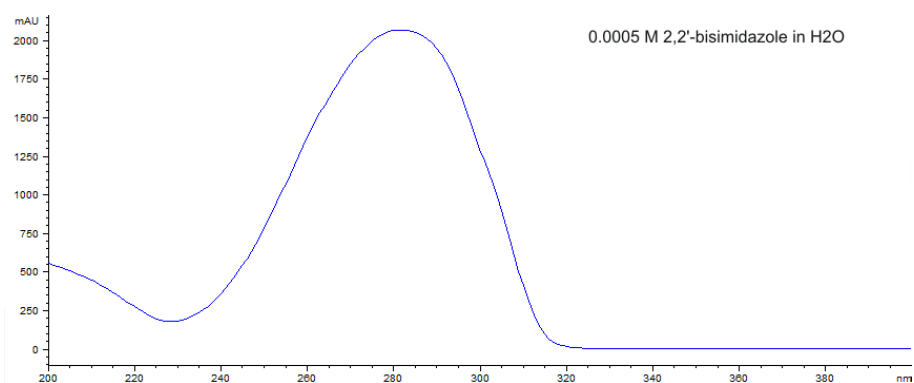


Figure S16: UV-Vis spectrum of BI

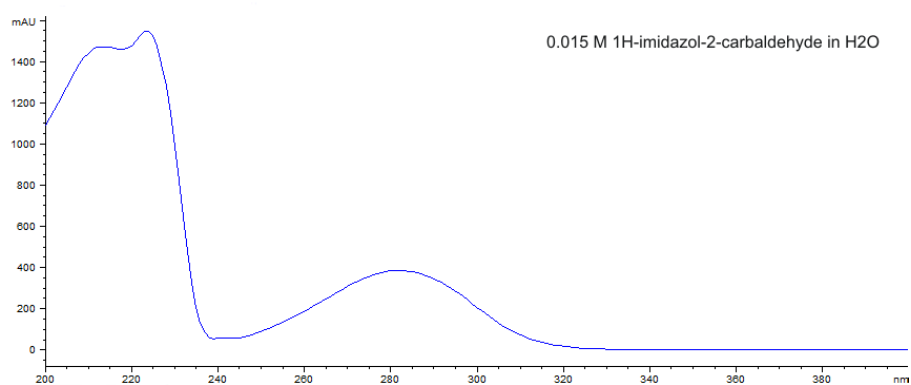


Figure S17: UV-Vis spectrum of IC

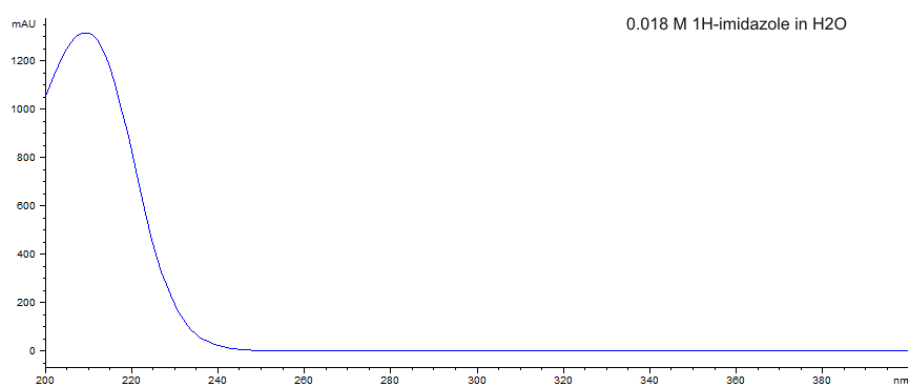


Figure S18: UV-Vis spectrum of IM